Karlsruhe Institute of Technology

www.lem.kit.edu
simon.hettler@kit.edu

Laboratory for Electron Microscopy

High-Resolution Transmission Electron Microscopy with Zach Phase Plate

S. Hettler[1], M. Dries[1], T. Schulze[1], M. Oster[2], C. Wacker[2], R. R. Schröder[2] and D. Gerthsen[1]

1. Laboratorium für Elektronenmikroskopie, Karlsruher Institut für Technologie, Engesserstr. 7, D-76131 Karlsruhe, Germany
2. BioQuant, CellNetworks, Universität Heidelberg, INF 267, D-69120 Heidelberg, Germany

Introduction

- Physical phase plates (PP) enhance the contrast of weak-phase objects in transmission electron microscopy (TEM) [1].
- Different methods exist to impose the required relative phase shift between scattered and unscattered electrons [2].
- A major disadvantage of the most common thin-film based PPs is the scattering of electrons in the PP itself leading to a phase-contrast damping and a loss of resolution.
- The electrostatic Zach-PP (Fig. 2) induces a variable phase shift on the unscattered electrons in the back focal plane (BFP) of the objective lens (Fig. 1) [3].
- As a damping or a loss of resolution is not expected, this work aims on the **application of the Zach-PP in high-resolution (HR)TEM.**

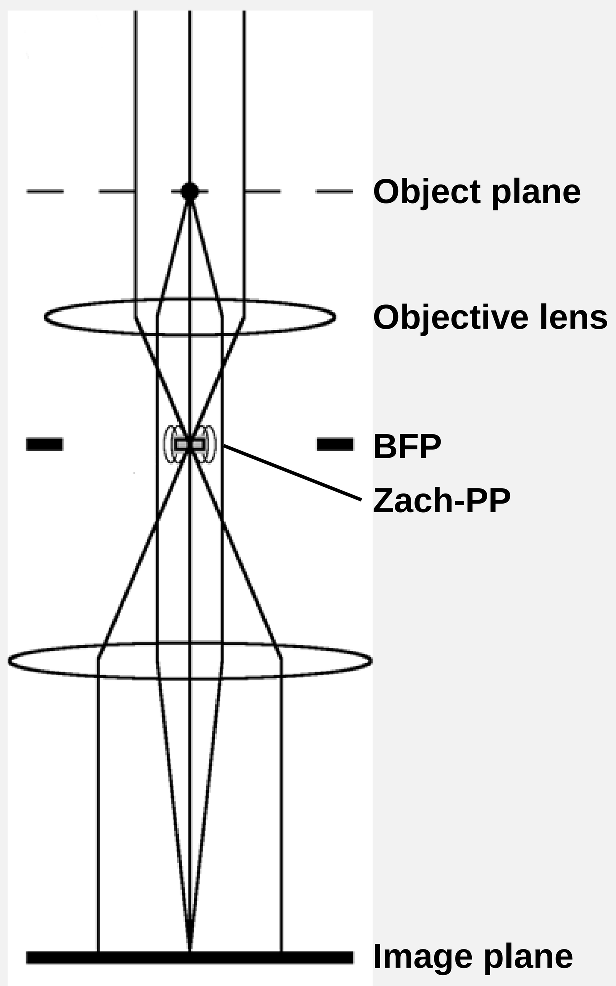

Fig. 1: Schematic illustration of an electrostatic Zach-PP positioned in the BFP of the objective lens.

Design and fabrication of a Zach-PP

- The Zach-PP consists of a single rod carrying a 5-layer system with Au electrode, insulating layers of Si_3N_4 and Al_2O_3 and Au shielding.
- Additional evaporation of amorphous carbon minimizes contamination and electrostatic charging.
- Complex fabrication process needed using electron-beam lithography, physical vapor deposition, reactive ion etching and focused ion beam milling as described in [4].
- Implementation in the BFP of a Zeiss 923Ω transmission electron microscope operated at 200 kV and equipped with a TVIPS CCD camera.

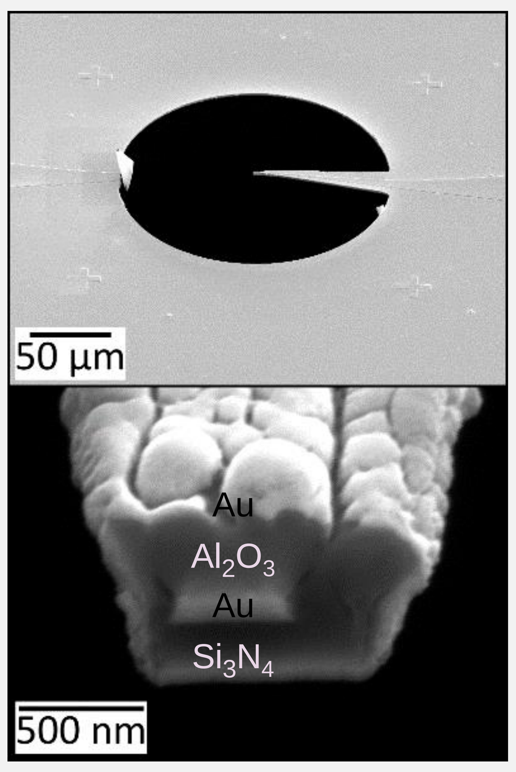

Fig. 2: Scanning electron microscopy images of the electrostatic Zach-PP used for the experiments. The detail image reveals the layer system.

Sample characterization

- Investigation of a Si single-crystal sample in [110] orientation.
- (111)-type lattice fringes and reflections are visible in the HRTEM image (Fig. 3a) and the corresponding power spectrum (Fig. 3b).

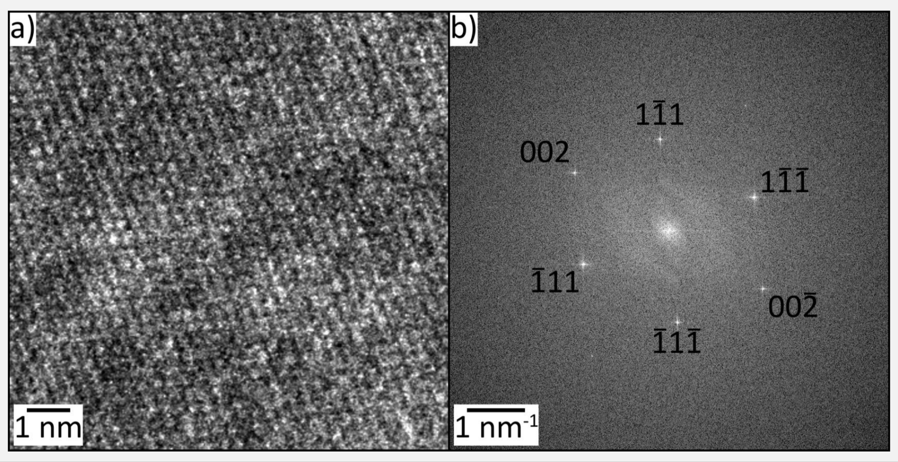

Fig. 3: Characterization of the Si single-crystal sample.
(a) Plan-view TEM image reveals (111)-type lattice fringes.
(b) The corresponding power spectrum shows the (111) and (002) reflections.

HRTEM image formation with Zach-PP

- The influence of the Zach-PP on the image formation process in HRTEM is best analyzed by the reflection intensity in power spectra.
- Assuming isotropic conditions, the reflection intensity $\tilde{I}$ shows a cosinusoidal dependence on the induced phase shift φ_{PP}.

$$\tilde{I}(u) \propto 2a_0 a_u E(u)|\cos(\varphi_u - \varphi_0 + \chi - \varphi_{PP})| \qquad \text{(Eq. 1)}$$

with the envelope function E ; the wave aberration function χ ;
the amplitude and phase of the diffracted/undiffracted beam $a_{u/0}$, $\varphi_{u/0}$
and the spatial frequency u.

Application of the Zach-PP

- Visibility of lattice fringes and reflections indicate a negligible phase-contrast damping induced by the Zach-PP (compare Figs. 3 and 4).
- (111) reflections are distinguished by their position with respect to the PP-rod (white): Affected (red) and unaffected (green).

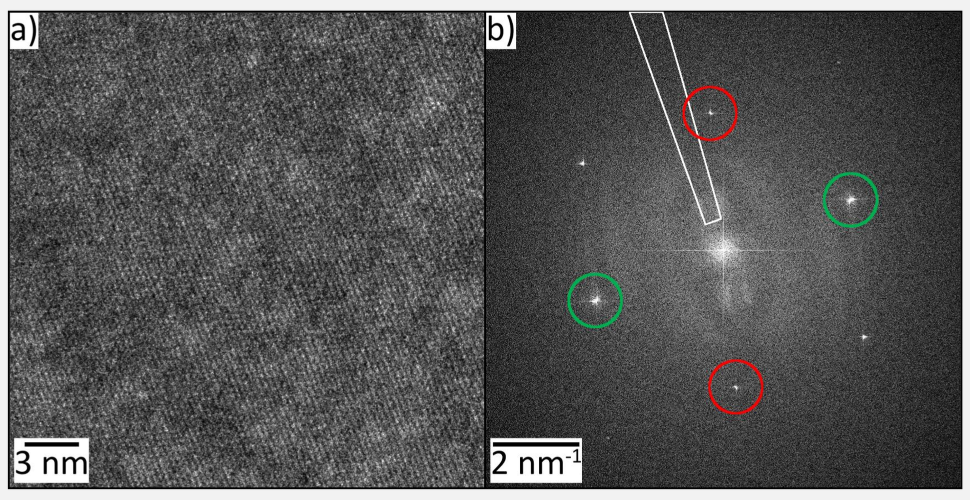

Fig. 4: HRTEM image of the Si single-crystal sample with Zach-PP.
(a) The visibility of the lattice fringes is an indication that the Zach-PP does not decrease the resolution.
(b) The corresponding power spectrum shows the marked (111) reflections and the rod of the Zach-PP.

Analysis of the reflection intensity

- Acquisition of a HRTEM image series of the same sample area with different applied voltages and otherwise unchanged conditions.
- A linear dependence of φ_{PP} on the applied voltage is verified by Thon-ring analysis.
- Determination of (111) reflection intensities in Wiener-filtered power spectra (x/+ in Fig.5).
- Fit to a function with cosinusoidal behavior (Eq. 1) yields a good agreement with the measured data points (Fig. 5).
- Undesired aberrations, charging effects or a deviation from perfect zone-axis orientation hamper the analysis and lead to the observed lower intensity of the (111) reflections affected by the PP rod (red curve in Fig. 5).

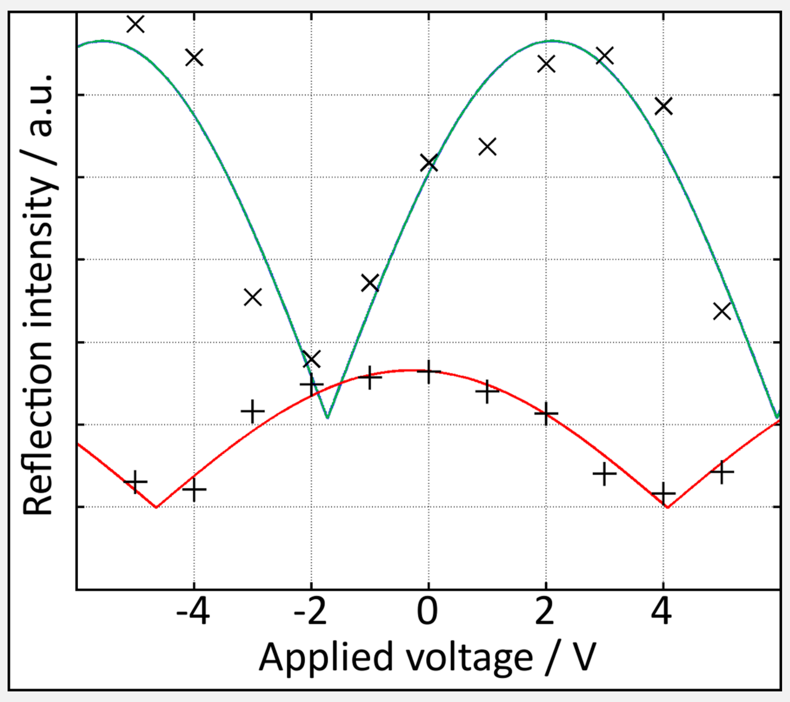

Fig. 5: Analysis of (111) reflection intensities in power spectra acquired with the Zach-PP in dependece of the applied voltage. Good agreement between measurements (x,+) and predicted cosinusoidal dependence (green, red curve).

Phase-contrast inversion in HRTEM images

- If one reflection is blocked by the PP rod, the HRTEM pattern is reduced to a line pattern (Fig. 6a), which is formed by the unaffected reflection pair (marked green in Fig. 6c).
- The remaining (111) reflection pair and the corresponding lattice fringe contrast can be influenced by φ_{PP}.
- The contrast of the lattice fringes can be inverted by applying appropriate PP-voltages, which is shown in the line profile in Fig. 6b taken from manually aligned images.

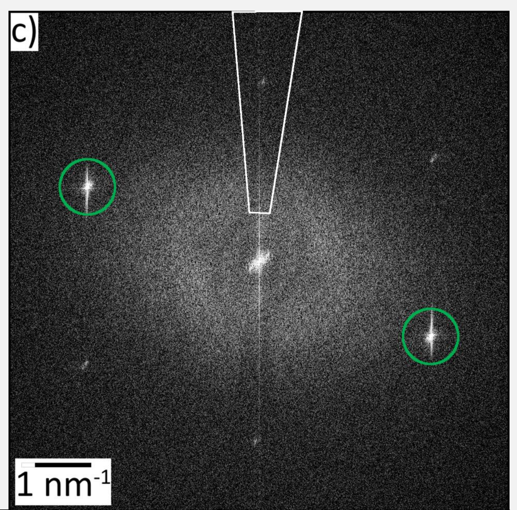

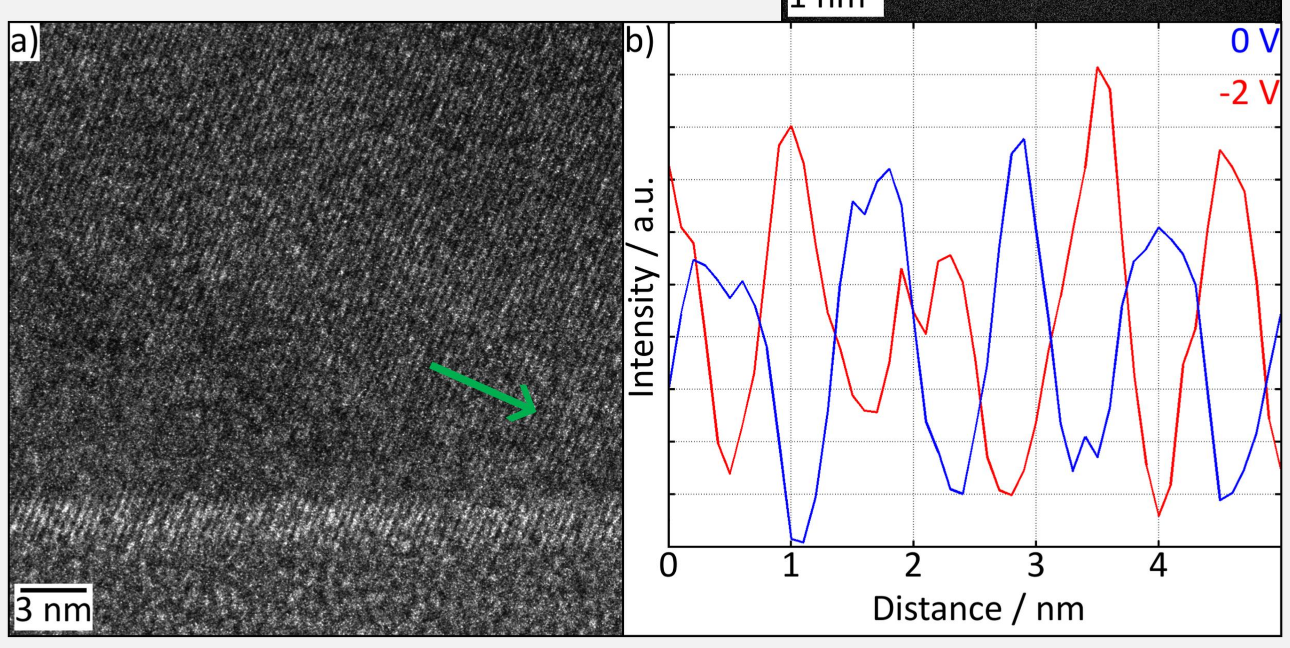

Fig. 6: Analysis of a HRTEM image with one reflection blocked by the PP.
(a) HRTEM pattern is reduced to a line pattern.
(b) Line profile across the green arrow in (a) shows inverted phase contrast for different applied voltages.
(c) Corresponding power spectrum to (a) shows the unaffected (111) reflection pair marked green.

Summary

- Application of the electrostatic Zach-PP for HRTEM is advantageous.
- Oscillation of the reflection intensity with varying φ_{PP}.
- Phase-contrast inversion of lattice fringes induced by the Zach-PP.
- Good agreement between experiment and theoretical calculations.

Outlook

- The application of the Zach-PP is limited by the capabilities of the microscope. Further investigation in a state-of-the-art microscope could offer:
- ➡ Determination of local information like sample thickness or composition.
- ➡ Quantitative HRTEM by object-wave reconstruction with Zach-PP [5].
- ➡ Improved resolution in single-particle reconstruction.

References

[1] R. Danev, K. Nagayama, *Ultramicroscopy* **88** (2001), p. 243-252.
[2] R. M. Glaeser, *Rev. Sci Instrum.* **84** (2013), 111101.
[3] K. Schultheiss et al., *Microsc. Microanal.* **16** (2010), p. 785-794.
[4] S. Hettler et al., *Microsc. Microanal.* **18** (2012), p. 1010-1015.
[5] B. Gamm et al., *Ultramicroscopy* **110** (2010), p. 807-814.
[6] Funding of the Deutsche Forschungsgemeinschaft is acknowledged.